

Weak Localization in Semiconductor Multi-Quantum Well Structures

F. G. Pikus

State University of New York, Stony Brook, NY 11794-3800

G. E. Pikus

A.F. Ioffe Physicotechnical Institute 194021 St Petersburg, RUSSIA

(March 24, 2022)

We have studied the phenomenon of weak localization in multi-quantum-well (MQW) structures in the regime of weak tunneling, when superlattice minibands are not formed. We have calculated the effect of weak localization on conductivity, which in this situation is described by a system of coupled Dyson equations. The tunneling across the MQW structure is found, in general, to suppress the weak localization effect on conductivity.

73.20.Fz, 71.70.Ej, 73.40.Kp, 71.55.Eq

The weak localization, which results from interference of two electron waves propagating along a closed path in opposite directions and manifests itself, among other effects, in the phenomenon of the negative magnetoresistance, has been studied extensively in metals and semiconductors, as well as thin films and quantum wells of these materials¹⁻⁴. Recently, a lot of attention has been devoted to studies of the weak localization in more complex systems, such as superlattices, multiple quantum wells, quantum wires, etc.⁵⁻⁷

The physics of the weak localization in the superlattices is of particular interest, and has been fairly extensively investigated, both theoretically⁵ and experimentally⁶. The theories vary in their approach, however, they all start from (implicit or explicit) assumption that the electron spectrum consists of well-defined minibands. This supposition is in fact equivalent to assuming that the tunneling time between two wells τ_{12} is much shorter than the momentum lifetime for in-plane motion, τ_{11} . This is a necessary condition for miniband formation, and for the structure to be treated as a superlattice.

The opposite case, when $\tau_{11} \ll \tau_{12}$ and an electron diffuses in a single quantum well for a long time before tunneling into a neighboring well, has never been studied, to the best of our knowledge. However, in practice both cases can be easily implemented, the first one - in a superlattice, the second one - in weakly coupled multiple quantum wells. In this latter case, there are no minibands, and no coherent motion across the planes of the MQW structure. The tunneling is sequential, i.e. there is no tunneling through many barriers at once, and tunneling into the next well does not depend on the history of electron motion.

We will be interested in the effects of such weak tunneling on the weak localization in lateral transport. Consequently, we choose the structure and make assumptions which help us to investigate this effect without additional

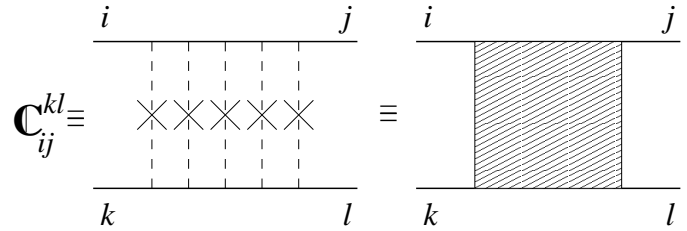


FIG. 1. Cooperon for multi-quantum-well structure, with indices i, j, k , and l denoting quantum well numbers.

complications. For example, we take the simple model for electron spin relaxation, which is described by the single spin-relaxation time $\tau_{SO} = \tau_{sxx} = \tau_{syy} = 2\tau_{szz}$ ⁸. From Refs. [9,10] one can see that in A_3B_5 quantum wells this approximation works quite well for large electron densities. We also assume that the temperature is low, $T \ll \epsilon_F$, and that $\hbar/\tau_{11}\epsilon_F \ll 1$ - the usual conditions in the theory of weak localization² (here ϵ_F is the electron Fermi energy).

The weak localization contribution to the conductivity of a single quantum well is given by the well-known expression^{3,4}:

$$\Delta\sigma_1 = -\frac{e^2 D}{\pi \hbar} \cdot 2\pi\nu_0\tau_{11}^2 \sum_{\alpha\beta} \int_0^{q_{\max}} \mathbf{C}_{\alpha\beta\beta\alpha}(\mathbf{q}) \frac{d^2 q}{(2\pi)^2}, \quad (1)$$

where

$\mathbf{C}(\mathbf{q})_{\alpha\beta\beta\alpha}$ is the Cooperon, α and β are the spin indices which we will omit in all subsequent expressions, $q_{\max}^2 = (Dt_1)^{-1}$, $D = v^2 t_1/2$ is the diffusion coefficient, t_1 is the transport time for in-plane motion in a well (differs from the lifetime τ_{11} for long-range scattering), and $\nu_0 = m/2\pi$ is the density of states at the Fermi level.

In the case of a MQW structure, the Cooperon is a 4-dimensional matrix indexed by the well numbers, \mathbf{C}_{ij}^{kl} (see Fig. 1). The total conductivity of the structure with N wells is

$$\Delta\sigma = \sum_{n=1}^N \Delta\sigma_n \quad (2)$$

$$= -\frac{e^2 D}{\pi \hbar} \cdot 2\pi \nu_0 \tau_{11}^2 \sum_{\alpha\beta} \int_0^{q_{\max}} \sum_{n=1}^N \mathbf{C}_{nn}(\mathbf{q}) \frac{d^2 q}{(2\pi)^2},$$

where $\mathbf{C}_{nn} \equiv \mathbf{C}_{nn}^{nn}$. For large number of wells N the calculations can be greatly simplified if we impose periodical boundary conditions, so the N -th well is connected with the 1st. We will also assume all wells to be identical. In this case

$$\Delta\sigma = N\Delta\sigma_1 \quad (3)$$

$$= -\frac{e^2 D}{\pi \hbar} \cdot 2\pi \nu_0 \tau_{11}^2 \sum_{\alpha\beta} \int_0^{q_{\max}} N \mathbf{C}_{11}(\mathbf{q}) \frac{d^2 q}{(2\pi)^2},$$

The Cooperon can be found from the Dyson equation, or, in our case, system of Dyson equations, since the component \mathbf{C}_{nm} is connected with $\mathbf{C}_{nm\pm 1}$. These equations are represented by diagrams shown in Fig. 2. Note that each “component” is actually a 4-dimensional $2 \times 2 \times 2 \times 2$ matrix with spin indices, which can alternatively be represented as a 4×4 matrix indexed by pairs $\alpha\beta$. These equations contain only components $\mathbf{C}_{1n} \equiv \mathbf{C}_{1n}^{1n}$, similar equations exist for components \mathbf{C}_{2n} and so on. There are, of course, other components of the Cooperon \mathbf{C}_{ij}^{kl} , however, none of them is relevant for the weak localization conductivity correction: some turn to 0 after averaging over impurities (like \mathbf{C}_{11}^{21} which contains $\langle V_{11} V_{21} \rangle = 0$, where V_{ij} is the matrix element for scattering with initial state in well i and final state in well j); other, while non-zero, do not contribute to the conductivity, (for example, the contribution of \mathbf{C}_{11}^{22} is proportional to the overlap of the wave functions in different wells, because lines 1 and 2 would have to meet in the vortex, and we assume that this overlap is extremely small). These ignored diagram also does not contribute in the Dyson equations, unless the scattering in the two wells is correlated, i.e. they do not couple with \mathbf{C}_{11} and \mathbf{C}_{12} as long as $\langle V_{11} V_{22} \rangle = 0$. Another component, \mathbf{C}_{12}^{21} , in principle can give contribution to the conductivity (just like its spin analog, $\mathbf{C}_{\alpha\beta}^{\beta\alpha}$, does give such contribution). However, in order for this component to be non-zero, there has to be at least one scattering act which occurs on the same scattering center but in different wells. We assume that the scattering centers have short enough range so there is no correlation in the scattering potentials in neighboring wells. Hence, there exists no such center which can scatter electrons in both wells, and the Cooperon component \mathbf{C}_{12}^{21} vanishes.

Written as a system of integral equations, Fig. 2 becomes

$$\begin{aligned} \mathbf{C}_{11}(\mathbf{q}) &= |V_{11}|^2 \\ &+ \int d^2 g_1 |V_{11}|^2 G_1^+(\omega, \mathbf{g}_1 + \mathbf{q}) G_1^-(\omega, -\mathbf{g}_1) \mathbf{C}_{11}(\mathbf{q}) \\ &+ \int d^2 g_2 |V_{12}|^2 G_2^+(\omega, \mathbf{g}_2 + \mathbf{q}) G_2^-(\omega, -\mathbf{g}_2) \mathbf{C}_{21}(\mathbf{q}) \end{aligned}$$

$$\begin{aligned} &+ \int d^2 g_N |V_{1N}|^2 G_N^+(\omega, \mathbf{g}_N + \mathbf{q}) G_N^-(\omega, -\mathbf{g}_N) \mathbf{C}_{N1}(\mathbf{q}), \\ \mathbf{C}_{21}(\mathbf{q}) &= |V_{21}|^2 \\ &+ \int d^2 g_1 |V_{21}|^2 G_1^+(\omega, \mathbf{g}_1 + \mathbf{q}) G_1^-(\omega, -\mathbf{g}_1) \mathbf{C}_{11}(\mathbf{q}) \\ &+ \int d^2 g_2 |V_{22}|^2 G_2^+(\omega, \mathbf{g}_2 + \mathbf{q}) G_2^-(\omega, -\mathbf{g}_2) \mathbf{C}_{21}(\mathbf{q}) \\ &+ \int d^2 g_3 |V_{23}|^2 G_3^+(\omega, \mathbf{g}_3 + \mathbf{q}) G_3^-(\omega, -\mathbf{g}_3) \mathbf{C}_{31}(\mathbf{q}), \end{aligned} \quad (4)$$

and so on for all the components \mathbf{C}_{n1} . Note that the tunneling is only possible between the neighboring wells, so only terms with $V_{n,n\pm 1}$ are present. Here $G^\pm(\omega, \mathbf{k})$ are the Green's functions,

$$G^\pm(\omega, \mathbf{k}) = \frac{1}{\omega - E(k) \pm i \left(\frac{1}{2\tau_{11}} + \frac{1}{2\tau_\varphi} \right)}, \quad (5)$$

$E(k) = k^2/2m$ and τ_φ is the phase relaxation time. After the integration by $E(g)$ in the right-hand side of Eq. (4) the result is expanded up to second order terms in series in small parameters τ_{11}/τ_φ and $\mathbf{v}\mathbf{q}\tau_{11}$ ($\mathbf{v} = \partial E/\partial \mathbf{k}$). Also, the Cooperon $\mathbf{C}_{ij}^{kl}(\mathbf{q})$ is expanded in harmonics:

$$\mathbf{C}_{ij}^{kl}(\mathbf{q}) = \sum_n C_{ij}^{kl(n)} \cos n\phi_{\mathbf{q}}, \quad (6)$$

where $\tan \phi_{\mathbf{q}} = q_y/q_x$. These transformations follow closely Refs. [2–4] and are described in details, for example, in Ref. [9]. Only the 0-th harmonic of the Cooperon, $C_{ij}^{kl} \equiv C_{ij}^{kl(0)}$, gives non-negligible contribution to the conductivity. For the components C_{n1} we arrive to the following system of linear equations:

$$\begin{aligned} C_{11} &= |V_{11}|^2 + \frac{\tau_0}{\tau_{11}} (1 - L_{11}\tau_0) C_{11} \\ &+ \frac{\tau_0}{\tau_{12}} (1 - L_{12}\tau_0) (C_{12} + C_{N1}), \\ C_{21} &= |V_{21}|^2 + \frac{\tau_0}{\tau_{11}} (1 - L_{11}\tau_0) C_{21} \\ &+ \frac{\tau_0}{\tau_{12}} (1 - L_{12}\tau_0) (C_{11} + C_{31}), \\ C_{31} &= \frac{\tau_0}{\tau_{11}} (1 - L_{11}\tau_0) C_{31} \\ &+ \frac{\tau_0}{\tau_{12}} (1 - L_{12}\tau_0) (C_{21} + C_{41}), \dots \end{aligned} \quad (7)$$

Here

$$\frac{1}{\tau_0} = \frac{1}{\tau_{11}} + \frac{2}{\tau_{12}},$$

τ_{11} is the momentum lifetime in a well, τ_{12} is a tunneling time between two neighboring wells:

$$\tau_{1n}^{-1} = 2\pi \nu_0 |V_{1n}|^2,$$

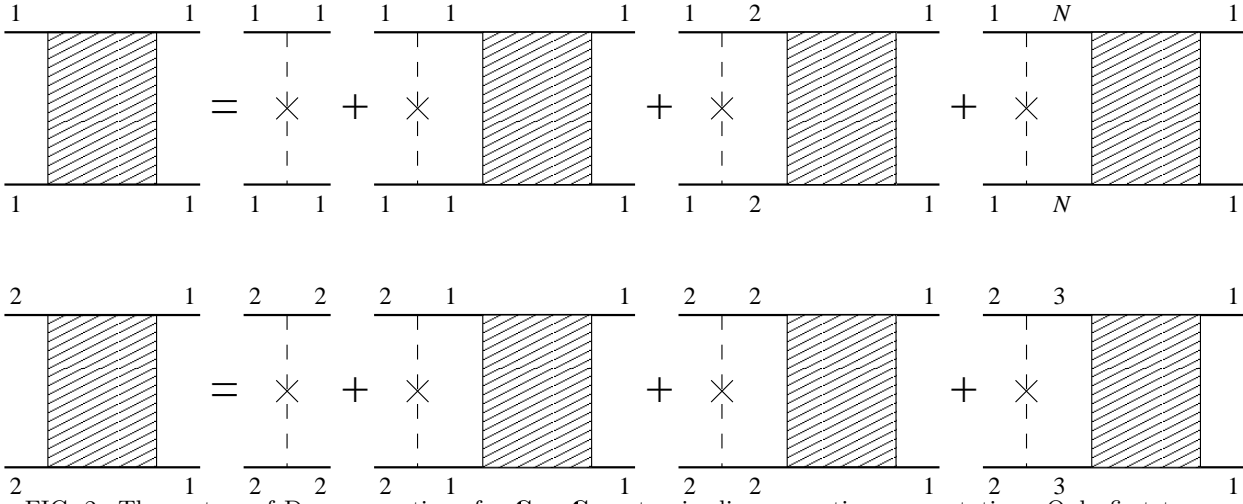


FIG. 2. The system of Dyson equations for \mathbf{C}_{11} , \mathbf{C}_{21} , etc. in diagrammatic representation. Only first two equations are shown.

and

$$L_{11} = L_{12} = L = Dq^2 + \frac{1}{\tau_\phi} + \frac{1}{\tau_{\text{SO}}} \quad (8)$$

is a 4×4 matrix, indexed, like the Cooperon itself, by pairs of spin indices $\alpha\beta$. In the basis of eigenfunctions of total momentum of the pair of electrons, singlet ϕ_0 and triplet ϕ_1^m with $m = -1, 0, 1$ this matrix becomes

$$L_0 = Dq^2 + \frac{1}{\tau_\phi}, \quad L_1^m = Dq^2 + \frac{1}{\tau_\phi} + \frac{1 + \delta_{m0}}{\tau_{\text{SO}}}, \quad (9)$$

where δ_{m0} is the δ -symbol.

The system (7) can be further simplified if we exploit the condition that $\tau_{12} \gg \tau_{11} \approx \tau_{11}$, and keep only terms of the first order in τ_{11}/τ_{12} (however, the product $L\tau_{12}$ can be large or small, and we make no assumptions about its magnitude here). We can also simplify the expressions by introducing

$$S(q) = 2\pi\nu_0\tau_{11}^2 C(q) \quad (10)$$

Then the system of linear equations for S_{1n} becomes

$$\begin{aligned} A_1 S_{11} + A_2 (S_{21} + S_{N1}) &= \tau_{11}, \\ A_1 S_{21} + A_2 (S_{11} + S_{31}) &= \tau_{12} \approx 0, \\ A_1 S_{31} + A_2 (S_{21} + S_{41}) &= 0, \dots \end{aligned} \quad (11)$$

where

$$\begin{aligned} A_1 &= \frac{\tau_0}{\tau_{12}} (2 + L\tau_{12}) \approx \frac{\tau_0}{\tau_{12}} (2 + x), \\ A_2 &= \frac{\tau_0}{\tau_{12}} (-1 + L\tau_0) \approx -\frac{\tau_0}{\tau_{12}}, \\ x &= L\tau_{12}. \end{aligned} \quad (12)$$

The system of linear equations (11) allows us to find $S_{11}(q)$ (which is a 4×4 matrix in the basis of singlet and triplet eigenfunctions ϕ_0, ϕ_1^m). The weak localization correction to the conductivity (3) can be expressed

through the eigenvalues of the inverse matrix, $S_{11}^{-1}(q)$, as follows^{11,12,9}:

$$\Delta\sigma = -\frac{e^2 D}{\pi\hbar} N \int_0^{q_{\text{max}}} \left(-\frac{1}{E_0} + \sum_{m=-1}^1 \frac{1}{E_1^m} \right) \frac{d^2 q}{(2\pi)^2}. \quad (13)$$

Here eigenvalue E_0 corresponds to the eigenfunction ϕ_0 , and E_1^m - to ϕ_1^m . Since the matrix L , and, hence, S_{11} , are diagonal in this basis, the eigenvalues E_0 and E_1^m of $S_{11}^{-1}(q)$ are just inverse of its corresponding diagonal elements, $(S_{11})_0$ and $(S_{11})_1^m$, respectively, and

$$\Delta\sigma = -\frac{e^2 D}{\pi\hbar} N \int_0^{q_{\text{max}}} \left(-S_0 + \sum_{m=-1}^1 S_1^m \right) \frac{d^2 q}{(2\pi)^2}. \quad (14)$$

Here we have omitted indices 11 of S to simplify the notation.

In a magnetic field B perpendicular to the planes of MQW the wave vector \mathbf{q} becomes an operator with the commutation relations

$$[q_+, q_-] = \frac{\delta}{D}, \quad \delta = \frac{4eBD}{\hbar c}, \quad (15)$$

where $q_{\pm} = q_x \pm iq_y$. This allows us to introduce creation and annihilation operators a^\dagger and a , respectively, for which $[aa^\dagger] = 1$:

$$D^{1/2} q_+ = \delta^{1/2} a, \quad D^{1/2} q_- = \delta^{1/2} a^\dagger, \quad Dq^2 = \delta\{aa^\dagger\}. \quad (16)$$

The non-zero matrix elements of these operators are

$$\begin{aligned} \langle n-1 | a | n \rangle &= \langle n | a^\dagger | n-1 \rangle = \sqrt{n}, \\ \langle n | \{aa^\dagger\} | n \rangle &= n + \frac{1}{2}. \end{aligned} \quad (17)$$

The integration over q in a magnetic field becomes summation over n , and the weak localization correction to the conductivity can be written as

$$\Delta\sigma = -\frac{e^2\delta}{4\pi^2\hbar}N \sum_{n=0}^{n_{\max}} \left(-S_{0n} + \sum_{m=-1}^1 S_{1n}^m \right). \quad (18)$$

where $n_{\max} = 1/\delta\tau_{11}$. It is convenient to extend the summation in Eq. (18) to $n \rightarrow \infty$. One can do it using the following transformation, which exploits the condition $n_{\max} \gg 1$ (this is the necessary condition for the diffusion approximation to work in the first place). We will see below that at large n the asymptotic values of S_{0n} and S_{1n}^m are $1/\delta n$. Therefore, the expression under the sum in Eq. (18) falls off as $2/\delta n$ and the sum diverges at large n . To remove this divergence we add and subtract $2/n+1$ to each term in Eq. (18): $\delta \sum_{n=0}^{n_{\max}} \left(-S_{0n} + \sum_{m=-1}^1 S_{1n}^m \right) = \sum_{n=0}^{n_{\max}} \left(-\delta S_{0n} + \delta \sum_{m=-1}^1 S_{1n}^m - \frac{2}{n+1} \right) + \sum_{n=0}^{n_{\max}} \frac{2}{n+1}$. The first sum can be extended to $n = \infty$ because the expression under the sum falls off as $1/n^2$ at large n . The second sum, again for $n_{\max} \gg 1$ can be approximated by $\ln n_{\max}$. Since the quantity of practical interest is not $\Delta\sigma$ itself but the magnetoconductivity $\Delta\sigma(B) - \Delta\sigma(0)$, which is measured experimentally, we can replace $\ln n_{\max} = \ln 1/\delta\tau_{11}$ by $\ln 1/\delta\tau_{\varphi}$ and ignore the B -independent term $\ln \tau_{\varphi}/\tau_{11}$. After these transformations, we arrive to the expression for the magnetoconductivity which does not contain τ_{11} at all:

$$\begin{aligned} \Delta\sigma(B) - \Delta\sigma(0) = & \quad (19) \\ & -\frac{e^2}{4\pi^2\hbar}N \left[\sum_{n=0}^{\infty} \left(-\delta S_{0n} + \delta \sum_{m=-1}^1 S_{1n}^m - \frac{2}{n+1} \right) \right. \\ & \left. - 2 \ln(\delta\tau_{\varphi}) \right]. \end{aligned}$$

The linear system (11) with coefficients Eq. (12) remains the same in a magnetic field, with L now being a function of n instead of q :

$$\begin{aligned} L_{0n} &= \delta \left(n + \frac{1}{2} \right) + \frac{1}{\tau_{\phi}}, \\ L_{1n}^m &= \delta \left(n + \frac{1}{2} \right) + \frac{1}{\tau_{\phi}} + \frac{1 + \delta_{m0}}{\tau_{\text{SO}}}, \end{aligned} \quad (20)$$

The solution of the system (11) can be written in the following form, for each n and each spin index l, m :

$$S \equiv S_{11} = \frac{1}{L} F_N(x), \quad (21)$$

where N is the number of wells in the MQW structure and $x = L\tau_{12}$. The function $F_N(x)$ can be found by solving the system (11) for any particular N . One can check by direct substitution that the following general expression is valid for any N :

$$\begin{aligned} F_N(x) &= \frac{1}{2}(-x)^{N/2} {}_2F_1 \left(\frac{1-N}{2}, 1 - \frac{N}{2}; 1 - N; -\frac{4}{x} \right) \\ &\times \sec \left(N \arccos \frac{\sqrt{-x}}{2} \right), \end{aligned} \quad (22)$$

where ${}_2F_1(a, b; c; z)$ is the Hypergeometric function. For practical purposes it is more convenient to represent $F_N(x)$ by a ratio of two polynomials:

$$F_N(x) = (x+4) \frac{\sum_{m=0}^{N/2} x^{N/2-m} \frac{N}{N-m} \binom{m}{N-m}}{\sum_{m=0}^{N/2-1} x^{N/2-m-1} \binom{m}{N-m-1}}, \quad \text{even } N, \quad (23)$$

$$F_N(x) = \frac{\sum_{m=0}^{(N-1)/2} x^{(N-1)/2-m} \binom{m}{N-m-1}}{\sum_{m=0}^{(N-1)/2} x^{(N-1)/2-m} \binom{m}{N-m}}, \quad \text{odd } N,$$

It is interesting to note that this expression has a very compact limit at $N \rightarrow \infty$. By expanding $F_N(1/y)$ for very large N in series around $y = 0$ one can see that the first N coefficients of the series do not change with increasing N . They are given by the following expression:

$$F_N \left(\frac{1}{y} \right) = \sum_{i=0}^{N-1} K_i y^i + \dots, \quad K_i = \frac{(-4)^i \Gamma(i + \frac{1}{2})}{\sqrt{\pi} n!}. \quad (24)$$

To obtain the limit $F_{\infty}(x)$ we extend the summation to infinity, and the sum can be written in a closed form:

$$F_{\infty}(x) = \frac{1}{\sqrt{1 + \frac{4}{x}}} \quad (25)$$

In the above derivation of $F_N(x)$ we have assumed the periodical boundary conditions, i.e. that electron can tunnel between the 1st and N th wells. While greatly simplifies the calculations, this condition becomes inaccurate for small N , and a more accurate solution is needed. If there is no periodical boundary conditions, each well gives a different contribution into the total conductivity (see Eq. 2)). The components of the cooperon C_{nn} can be found from N systems of linear equations, system number m is written for coefficients $C_{1m}, C_{2m}, \dots, C_{Nm}$, and is similar to Eq. 7 but does not contain the tunneling between 1st and N th wells. From these systems we can find the components of the Cooperon C_{nn} , or S_{nn} , the sum of which enters the expression for conductivity. We can define an ‘‘average’’ S_{11}^* to be used instead of S_{11} in the above expressions for conductivity, and, similarly to Eq. (21), introduce function $F_N^*(x)$:

$$S^* = 1/N \cdot \sum_{n=1}^N S_{nn} = \frac{1}{L} F_N^*(x). \quad (26)$$

Figure 3 shows the function $F_N^*(x)$ for different number of wells N , from 2 to infinity. For large N , the difference between $F_N^*(x)$ and $F_N(x)$ is negligible, and the

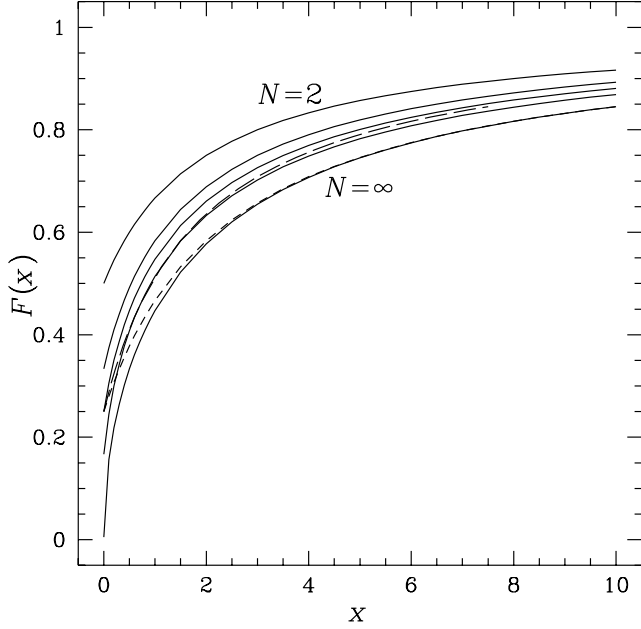


FIG. 3. Function $F_N^*(x)$, which determines Cooperon components entering the expressions for conductivity (see Eq. (21)) for $N = 2, 3, 4, 6$, and $N = \infty$ (solid curves, from highest to lowest). All functions shown by solid curves are obtained without using periodical boundary conditions. Using these boundary conditions for $N = 4$ results in $F_4(x)$ shown by short-dash line. Note that the periodical boundary conditions become much more accurate if the x axis is scaled by $(N - 1)/N$ (for the case of $N = 4$, shown by long-dashes line, the abscissae axis was scaled by $3/4$).

two coincide exactly for $N = \infty$. However, for small N , the periodical boundary conditions introduce a noticeable error; for example, in Fig. 3 we compare the functions $F_4^*(x)$ and $F_4(x)$ (short-dashed curve). It is interesting to note that replacing τ_{12} by an “effective” tunneling time $\tau'_{12} = N/(N - 1) \cdot \tau_{12}$ (or x by $x' = N/(N - 1) \cdot x$) makes the function $F_N(x')$ almost coincide with $F_N^*(x)$. The reason for this behaviors is intuitively clear: by applying periodic boundary conditions we have added an “extra” tunneling link to the structure, in addition to the $N - 1$ “real” links. Scaling τ_{12} makes the “cumulative” tunneling rate for the structure with periodical boundary conditions equal to that of the real structure. For $N = 2$ this procedure, obviously, gives exactly correct function, since the periodic boundary conditions at $N = 2$ are equivalent to just doubling the tunneling rate. In Fig. 3 we show by the long-dashed curve the scaled function $F_4(4/3x)$; one can see that it looks very similar to $F_4^*(x)$.

We now have all the necessary expressions, namely, Eqs. (19, 20, 21, 23), to calculate the magnetoconductivity due to the weak localization in an MQW structure. First, following [11,12] we introduce the characteristic magnetic fields¹³

$$\begin{aligned} H_\varphi &= \frac{c\hbar}{4eD\tau_\varphi}, \quad \frac{B}{H_\varphi} = \delta\tau_\varphi, \\ H_{\text{SO}} &= \frac{c\hbar}{4eD\tau_{\text{SO}}}, \quad \frac{H_\varphi}{H_{\text{SO}}} = \frac{\tau_{\text{SO}}}{\tau_\varphi}, \\ H_{12} &= \frac{c\hbar}{4eD\tau_{12}}, \quad \frac{H_\varphi}{H_{12}} = \frac{\tau_{12}}{\tau_\varphi}. \end{aligned} \quad (27)$$

and dimensionless conductivity *per one quantum well*:

$$\delta\sigma(B) = \frac{2\pi\hbar}{Ne^2} [\Delta\sigma(B) - \Delta\sigma(0)]. \quad (28)$$

We begin by analyzing two limiting cases of weak and strong tunneling, or $x \gg 1$ and $x \ll 1$, respectively. In the first case we can immediately see from Eq. (24) that $F_N(\infty) = 1$, so $S = 1/L$ (note that at large n we also have $x \gg 1$ and, therefore, $S = 1/L \sim 1/\delta n$). Substituting expressions for L from Eq. (20) we obtain the standard result for single quantum well²:

$$\begin{aligned} \delta\sigma(B) &= \frac{1}{2\pi} \left[-\Psi\left(\frac{1}{2} + \frac{H_\varphi}{B}\right) + 2\Psi\left(\frac{1}{2} + \frac{H_\varphi}{B} + \frac{H_{\text{SO}}}{B}\right) \right. \\ &\quad \left. + \Psi\left(\frac{1}{2} + \frac{H_\varphi}{B} + \frac{2H_{\text{SO}}}{B}\right) - 2\ln\left(\frac{H_\varphi}{B}\right) \right], \end{aligned} \quad (29)$$

where Ψ is the digamma-function. This is not surprising since $x \rightarrow \infty$ corresponds to $\tau_{12} \rightarrow \infty$ in which case the parallel wells become completely independent. In the opposite case, $x \rightarrow 0$, we have from Eq. (23) that $F_N(0) = 1/N$, so $NS = 1/L$ and we again obtain the classical result, only now for the entire MQW structure since the tunneling couples the wells so that they all act as one well.

We now present the results of our calculations of the weak localization correction to the conductivity in multiple quantum wells for various parameters: number of wells N , spin relaxation time τ_{SO} , and tunneling time τ_{12} . We begin by analyzing the dependence of the dimensional magnetoconductivity $\delta\sigma(B)$ on the number of wells N , which is shown in Fig. 4 for $H_{\text{SO}}/H_\varphi = 2$ (this value is typical for A_3B_5 quantum wells, see Ref. [9]), $H_{12}/H_\varphi = 4$, and N from 2 to infinity. This figure also shows the effect of periodical boundary conditions at small N : the magnetoconductivity calculated with such boundary conditions for $N = 4$ is shown by a dashed curve. One can see that increasing the number of wells makes the minimum on the magnetoconductivity curve less pronounced. It is known^{11,12} that increasing τ_{SO} has similar effect on the magnetoconductivity, the minimum becomes less pronounced and eventually disappears as τ_{SO} increases; we illustrate this effect in the insert of Fig. 4 where $\delta\sigma(B)$ is shown for $N = 2$, $H_{12}/H_\varphi = 4$, and $H_{\text{SO}}/H_\varphi = 1/2$ (top curve), $H_{\text{SO}}/H_\varphi = 2$ (middle curve), and $H_{\text{SO}}/H_\varphi = 3$ (the lowest curve). One can say that coupling the wells tighter effectively makes the spin relaxation slower.

This similarity between effects of increasing number of wells and increasing τ_{SO} is not complete: one can see

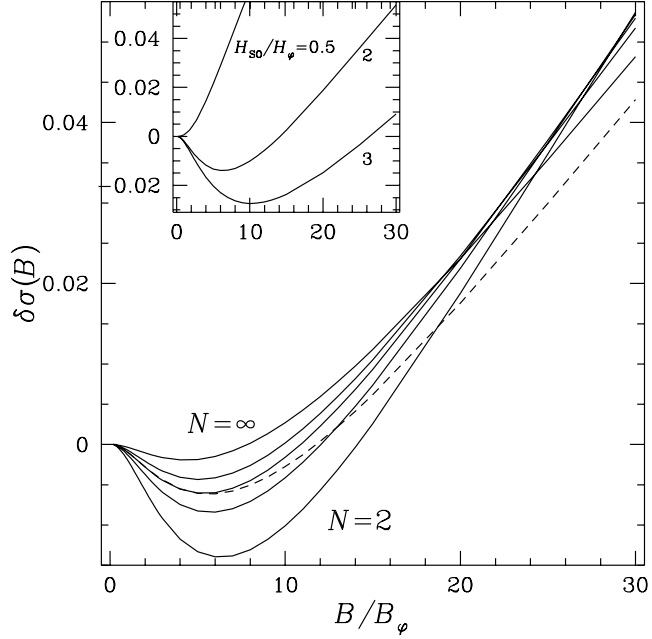


FIG. 4. Dimensionless magnetoconductivity $\delta\sigma(B)$ for $H_{SO}/H_\varphi = 2$ and $H_{12}/H_\varphi = 4$ and different number of wells $N = \infty, 6, 4, 3$, and $N = 2$ (solid lines, in order from higher to lower near the minimum). The solid lines were calculated without using the periodical boundary conditions. The magnetoconductivity calculated with these conditions is shown for $N = 4$ by a dashed line. The inset shows the effect of spin relaxation on magnetoconductivity for $N = 2$ and $H_{12}/H_\varphi = 4$.

from Fig. 4 that the minimum on the magnetoconductivity curve does not disappear as N increases, while increasing τ_{SO} leads to a monotonic $\delta\sigma(B)$. After studying the dependencies of $\delta\sigma(B)$ on all the parameters, we have found that if for a given τ_{SO} and some N , τ_{12} the function $\delta\sigma(B)$ has a minimum, this will not change for any other N and τ_{12} as long as τ_{SO} is maintained the same. To better understand this behavior, we examine the magnetoconductivity dependence on τ_{12} . Figure 5 shows the magnetoconductivity for $N = 3$, $H_{SO}/H_\varphi = 2$, and H_{12}/H_φ from 0 to 100. From the analysis of the limiting cases $\tau_{12} \ll \tau_\varphi$ and $\tau_{12} \gg \tau_\varphi$ we can conclude that

$$\delta\sigma(B, \tau_{12} = \infty) = N\delta\sigma(B, \tau_{12} = 0). \quad (30)$$

It is obvious that both limiting cases are either monotonic, or not. From Fig. 5 one can see that, while it is not true that all $\delta\sigma(B, \tau_{12})$ curves are contained between these two limits, the minimum is present on all of the curves.

The situation at $N = \infty$ is slightly different, since from the analysis of the limiting cases and Eq. (30) it follows that the conductivity “per one well” $\delta\sigma$ tends to 0 at small τ_{12} (the conductivity of the entire system is, of course, infinite for any $\tau_{12} > 0$). Therefore, with decreasing τ_{12} the magnetoconductivity also decreases, as demonstrated in Fig. 6. However, the main qualitative

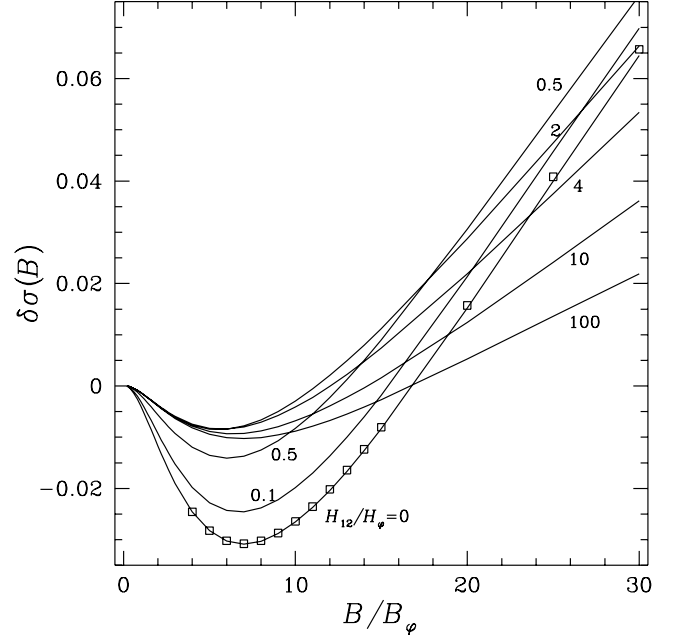


FIG. 5. Dimensionless magnetoconductivity $\delta\sigma$ for $N = 3$, $H_{SO}/H_\varphi = 2$, and H_{12}/H_φ from 0 to 100. The squares show $3 \cdot \delta\sigma(B, H_{12}/H_\varphi = 100)$ (which is very close to the limit at $H_{12} = \infty$), to illustrate the connection Eq. (30) between magnetoconductivity at $H_{12} = 0$ and $H_{12} = \infty$.

features of the magnetoconductivity dependence on tunneling remain the same: if the minimum of $\delta\sigma$ exists with no tunneling, it also exists at any tunneling rate. The inset shows that the opposite is also true: if the dependence $\delta\sigma(B)$ was monotonic for $\tau_{12} = \infty$, it remains so for any finite τ_{12} .

In conclusion, we have analyzed the effect of weak tunneling between quantum wells in a multi-quantum-well structure on the weak localization and the magnetoconductivity caused by it. We have found an analytical solution of the problem for the case when spin relaxation can be described by a single spin relaxation time, neglecting the effects of the linear terms in spin relaxation Hamiltonian. The tunneling across the MQW structure was found to decrease the overall magnitude of the weak localization correction. However, it does not change the qualitative character of the magnetoconductivity, namely, presence (or absence) of regions of positive and negative magnetoconductivity. Our results show that the weak localization correction to the conductivity in multi-quantum-well structures is sensitive to the tunneling time τ_{12} and it should be possible to determine this time experimentally from the magnetoconductivity measurements.

G. E. P. acknowledges support by RFFI Grant 96-02-17849 and by the Volkswagen Foundation.

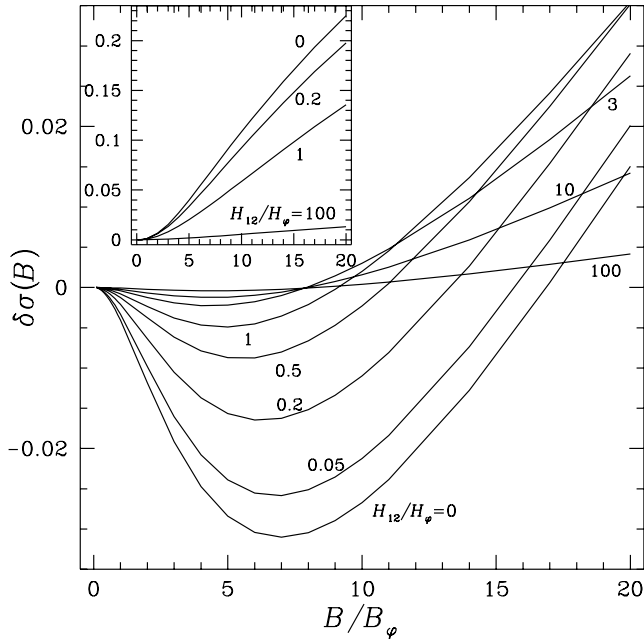


FIG. 6. Dimensionless magnetoconductivity $\delta\sigma$ for $N = \infty$, $H_{50}/H_\varphi = 2$, and H_{12}/H_φ from 0 to 100. The inset shows magnetoconductivity for $H_{50}/H_\varphi = 0.5$.

- ¹ B. L. Altshuler and A. G. Aronov, in “*Electron-Electron Interactions in Disordered Systems*”, p. 1; P. A. Lee and T. V. Ramakrishnan, Rev. Mod. Phys. **57**, 287 (1985); H. Fukuyama, in “*Electron-Electron Interactions in Disordered Systems*”, p. 155.
- ² B. Altshuler, D. Khmelnitskii, A. Larkin and P. Lee, Phys. Rev. B **22**, 5142 (1980).
- ³ S. Hikami, A. Larkin, and Y. Nagaoka. Progr. Theor. Phys. **63**, 707 (1980).
- ⁴ B. L. Altshuler, A. G. Aronov, A. I. Larkin, and D. E. Khmelnitskii, JETP **54**, 411 (1981) (JETP **81**, 788 (1981)).
- ⁵ W. Szott, C. Jedrzejek, W. P. Kirk, Phys. Rev. B **46** 15905 (1992); W. Szott, C. Jedrzejek, W. P. Kirk, Phys. Rev. B **40** 1790 (1989); W. Szott, C. Jedrzejek, W. P. Kirk, Phys. Rev. Lett. **63** 1980 (1989);
- ⁶ T. Schmidt *et. al*, Phys. Rev. B **54**, 13980 (1995); V. A. Kulbachinskii, V. G. Kutin, T. S. Babushkina, and I. G. Malkina, Brazilian Journal of Physics **26**, 313 (1996); V. A. Kulbachinskii *et. al*, Journal of Low Temperature Physics **102**, 499 (1996); E. L. Carpi and M. Van Hove, Superlattices and Microstructures **14**, 53 (1993)
- ⁷ P. E. Selbman, M. Suhrke, Solid State Electronics **37**, 717 (1994); C.-T. Liang *et. al*, in “*22nd International Conference on the Physics of Semiconductors*”, ed. by D. J. Lockwood, Singapore, World Scientific, vol. **2**, p. 1063; C.-T. Liang *et. al*, Phys. Rev. B **49**, 8518 (1994); K. Tsukagoshi *et. al*, Superlattices and Microstructures **16**, 295 (1994); G. M. Gusev *et. al*, Solid State Communications **85**, 317 (1993).
- ⁸ It was shown that for A_3B_5 quantum wells, where the spin relaxation occurs primarily via spin precession due to spin-orbit terms in the crystal Hamiltonian, the effects of spin

relaxation on the weak localization, in general, cannot be described by a single relaxation time (and if they can, the time measured from weak localization will almost certainly be very different from the results of other, more direct measurements, such as optical orientation experiments). The description which uses single spin relaxation time is valid for metal films². For A_3B_5 quantum wells it can only be applied in special cases; see Refs. 11,12,9,14,10.

- ⁹ W. Knap *et. al*, Phys. Rev. B. **53**, 3912 (1996).
- ¹⁰ T. Hassenkam *et. al*, Phys. Rev. B. **55**, 9233 (1997);
- ¹¹ S. V. Iordanskii, Yu. B. Lyanda-Geller, and G. E. Pikus, JETP Letters **60**, 206 (1994) (Pisma v JETP **60**, 199 (1994)).
- ¹² F. G. Pikus and G. E. Pikus, Phys. Rev. B. **51**, 16928 (1995).
- ¹³ An important note is in order here: our analysis explicitly assumes that the tunneling time between two wells τ_{12} is the same for all types of diffusion trajectories and all magnetic fields. This is obviously the case if the tunneling barriers are perfectly uniform. However, in most practical cases the tunneling through a barrier actually occurs in few “weak spots”, where the barrier is more transparent (see M. E. Raikh and I. M. Ruzin, in “*Hopping and Related Phenomena*”, ed. by H. Fritzsche and M. Pollak, Singapore: World Scientific, 1990, p. 217-41). In this case, different trajectories may have different probabilities of passing over such “weak spot” and τ_{12} will no longer be constant. Study of this effect presents a separate and fairly complex problem, which falls outside of the scope of this work.
- ¹⁴ F. G. Pikus and G. E. Pikus, Solid State Commun., **100**, 95 (1996).